NASA Technical Memorandum 100095

Computational Fluid Dynamics Drag Prediction–Results from the Viscous Transonic Airfoil Workshop

Terry L. Holst

(NASA-TM-100095) COMPUTATIONAL FLUID DYNAMICS DRAG PREDICTION: RESULTS FROM THE VISCOUS TRANSONIC AIRFOIL WORKSHOP (NASA) 15 p CSCL 01A G3/02

N88-22009

Unclas 0140254

April 1988

National Aeronautics and Space Administration

NASA Technical Memorandum 100095

Computational Fluid Dynamics Drag Prediction–Results from the Viscous Transonic Airfoil Workshop

Terry L. Holst, Ames Research Center, Moffett Field, California

April 1988

National Aeronautics and
Space Administration

Ames Research Center
Moffett Field, California 94035

COMPUTATIONAL FLUID DYNAMICS DRAG PREDICTION–RESULTS FROM THE VISCOUS TRANSONIC AIRFOIL WORKSHOP

Terry L. Holst *
NASA Ames Research Center, Moffett Field, California

ABSTRACT

Results from the Viscous Transonic Airfoil Workshop held in January 1987, are compared with each other and with experimental data. Test cases used include attached and separated transonic flows for the NACA 0012 airfoil. A total of 23 sets of numerical results from 15 different author groups are included. The numerical methods used vary widely and include: 16 Navier-Stokes methods, 2 Euler/boundary-layer methods, and 5 potential/boundary-layer methods. The results indicate a high degree of sophistication among the numerical methods with generally good agreement between the various computed and experimental results for attached or moderately separated cases. The agreement for cases with larger separation is only fair and suggests additional work is required in this area.

INTRODUCTION

During the past 3 years the Viscous Transonic Airfoil (VTA) Workshop was planned, organized, and implemented. The workshop implementation was in two parts. The first part consisted of presentations at the AIAA 25th Aerospace Sciences Meeting at Reno, Nevada, in January 1987 by 15 author groups with a variety of different viscous airfoil numerical methods (Refs. 1-16). The second part of the VTA Workshop was the presentation of a compendium of results (Ref. 17) where the individual contributions were combined in a format to facilitate comparisons among both the various computations and selected experimental data. In this paper results from the VTA workshop obtained for the NACA 0012 airfoil are reexamined and analyzed with special emphasis on drag.

The individual author groups have computed a set of results for test cases involving a variety of different situations ranging from attached subcritical flows to transonic flows with both shock-induced and angle-of-attack induced separation. A complete set of instructions given to each author group, which lists all of the requested airfoil cases, required results, and result format, is reproduced in Ref. 17.

The methods used by the various authors vary from momentum-integral boundary-layer methods coupled with transonic potential inviscid codes to full Navier-Stokes methods. A quick-reference table showing authors, paper references, and methods used is given in Table 1. A total of 23 different sets of results were submitted by the 15 author groups as several authors decided to submit several sets of results. The majority of methods (a total of 16) utilize the Navier-Stokes equations. This is in direct contrast to the situation in 1980-81 at the Stanford Workshop on Complex Turbulent Flows (Ref. 18) where very limited results on airfoil calculations were submitted with Navier-Stokes methods. This suggests a strong trend toward the Navier-Stokes formulation, even though it can be computationally expensive. The remaining formulations are split between several categories: two are Euler/boundary-layer methods, and five are potential/boundary-layer methods. The boundary layer methods are divided between the momentum integral approach and the full boundary layer equation approach.

Major objectives to be addressed in this paper include the establishment of the abilities of viscous airfoil analysis methods to predict aerodynamic trends including drag and the establishment of the quantitative abilities of the various methods for predicting details of viscous airfoil flow fields. In short, the primary objective of this paper is CFD computer code validation. There are two types of errors which the validation process seeks to identify and hopefully eliminate. These include physical model errors and numerical errors. The physical models associated with CFD applications include the governing equations, the viscosity law, boundary conditions, the equation of state, and the turbulence model. Numerical errors associated with CFD applications are due to time and space discretization schemes, boundary condition implementation schemes, grid resolution, grid stretching, and artificial dissipation. Differences between two computed results that use different physical models are best evaluated by using accurate experimental data. Differences between two computed results that use the same physical models have to be numerical in nature by definition. Numerical errors can be effectively identified by numerical solution-to-solution comparisons. Grid refinement studies, outer boundary position studies, and code-to-code comparisons are examples of this type of error evaluation scenario. In actual practice physical model and numerical errors coexist in most applications. Thus, identification, evaluation, and removal of errors associated with CFD applications are best accomplished by a combined implementation of experimental and solution-to-solution comparisons. The purpose of the VTA Workshop in general, and this paper in particular, is to achieve this type of comprehensive code validation for the viscous transonic airfoil problem.

DISCUSSION OF RESULTS

The NACA 0012 airfoil is a symmetric, 12% thick airfoil which has an analytical definition given in Ref. 17. This airfoil, while not being state of the art in airfoil design, is extremely valuable as a standard because it has been tested extensively both experimentally and computationally. As a consequence, a range of experimental results taken from various sources can be compared with the present range of computational results.

* Chief, Applied Computational Fluids Branch.

Table 1 Summary of authors and numerical methods used in the Viscous Transonic Airfoil Workshop.

no.	author(s)[ref]	method description
1	Sugavanam[1]	NS, modified ADI, BL
2	Desai,Rangarajan[2]	NFP+LEBL+visc ramp, SLOR+grid sequencing
3	Dargel,Thiede[3]	NFP+MIBL+nonisentropic shock-point operator
4	Rumsey,Taylor,Thomas Anderson[4]	NS, AF, upwind FV, BL
5	Melnik,Brook,Mead[5]	CFP+LEBL, MG-ADI
6	Maksymiuk, Pulliam[6]	NS, diagonal-ADI, BL
7	Coakley[7]	NS, upwind-ADI, FV, CS
8	"	NS, upwind-ADI, FV, BL
9	"	NS, upwind-ADI, FV, JK
10	"	NS, upwind-ADI, FV, (q-ω)
11	Chen,Li,Alemdavoglu Mehta,Chang,Chen, Cebeci[8,9]	Euler+IBL, MG, FV, CS
12	"	NS, ADI, BL
13	"	FP+IBL, CS
14	King[10]	NS, ADI, CS
15	"	NS, ADI, BL
16	"	NS, ADI, JK
17	Huff, Wu, Sankar[11]	NS, ADI, BL
18	Matsushima, Obayashi, Fujii[12]	NS, LU-ADI, flux limiter, BL
19	Haase, Echtle[13]	NS, 3-step RK+RA, FV, CS
20	"	CFP+LEBL, MG-ADI
21	Kordulla[14]	NS, implicit pred-corr, BL
22	Drela, Giles[15]	Euler+MIBL, FV, Newton it
23	Morinishi,Satofuka[16]	NS, MG, RK, RA, BL

NS–Navier-Stokes, NFP–nonconservative full potential, CFP–conservative full potential, IBL–inverse boundary layer, LEBL–lag entrainment boundary layer, MIBL–momentum integral boundary layer, MG–multigrid, FV–finite volume, RK–Runge-Kutta, RA–residual averaging, BL–Baldwin-Lomax, JK–Johnson-King, CS–Cebeci-Smith

The first results for the NACA 0012 airfoil are pressure coefficient distributions at $M_\infty = 0.7$, $\alpha = 1.49°$, and $Re_c = 9\text{x}10^6$. These results, including 20 separate curves, are presented in Fig. 1 on a single set of axes without labels. For this case the flow is attached and just slightly supersonic near the leading edge upper surface. All methods produce very similar results with very little scatter and are in excellent agreement with the experimental data of Harris (Ref. 19). The measured experimental angle of attack for this case was 1.86°. Using a linear method for simulating wind-tunnel-wall interference, Harris determined the corrected angle of attack to be 1.49°. This is the angle of attack used to compute all the results displayed in Fig. 1. The consistency and accuracy of results for this case indicate that, at least for surface pressure associated with attached, weakly transonic flow, computational methods have attained a sophisticated level of development.

The second set of results computed for the NACA 0012 airfoil also consist of pressure coefficient distributions and are displayed in Fig. 2. These calculations were performed for $M_\infty = 0.55$, $\alpha = 8.34°$, and $Re_c = 9\text{x}10^6$. Again the angle of attack used in the computations (8.34°) is the corrected value obtained by Harris from the measured value (9.86°) using a linear analysis for wind-tunnel-wall effects. For this case the flow has a supersonic bubble well forward on the airfoil upper surface and is slightly separated at the foot of the shock. In addition, several authors reported boundary layer separation at the airfoil trailing edge. The angle of attack for this case is about one degree below the maximum lift value.

The computed results for this case are displayed in two different plots (all without labels). Computations utilizing inviscid-plus-boundary-layer methods (6 curves) are displayed in Fig. 2a, and computations utilizing Navier-Stokes methods (16 curves) are displayed in Fig. 2b. Both sets of computations are in good agreement with Harris' experimental data. However, the inviscid-plus-boundary-layer results show considerably more scatter for this case than the Navier-Stokes results. Most of the scatter is associated with the solution near the airfoil leading edge on the upper surface, where the large angle of attack causes a rapid expansion followed almost immediately by a shock wave. Perhaps the generally coarser streamwise spacing of the inviscid grids used in the inviscid-plus-boundary-layer methods, which averaged 137 points relative to an average of 243 points for the Navier-Stokes methods, is inadequate to capture the large gradients associated with the inviscid flow at the airfoil leading edge. The two solutions that significantly underpredict the peak $-c_p$ level at the upper surface leading edge (one result from Fig. 2a and one result from Fig. 2b) are from very coarse-grid calculations, and therefore, tend to support this observation.

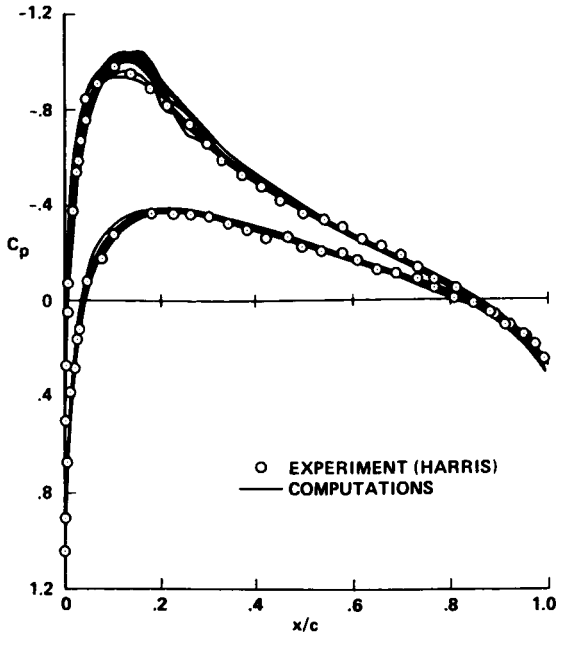

Fig. 1.- Comparison of pressure coefficient distributions for the NACA 0012 airfoil, $M_\infty = 0.70$, $\alpha = 1.49°$ (corrected), $Re_c = 9.0 \times 10^6$.

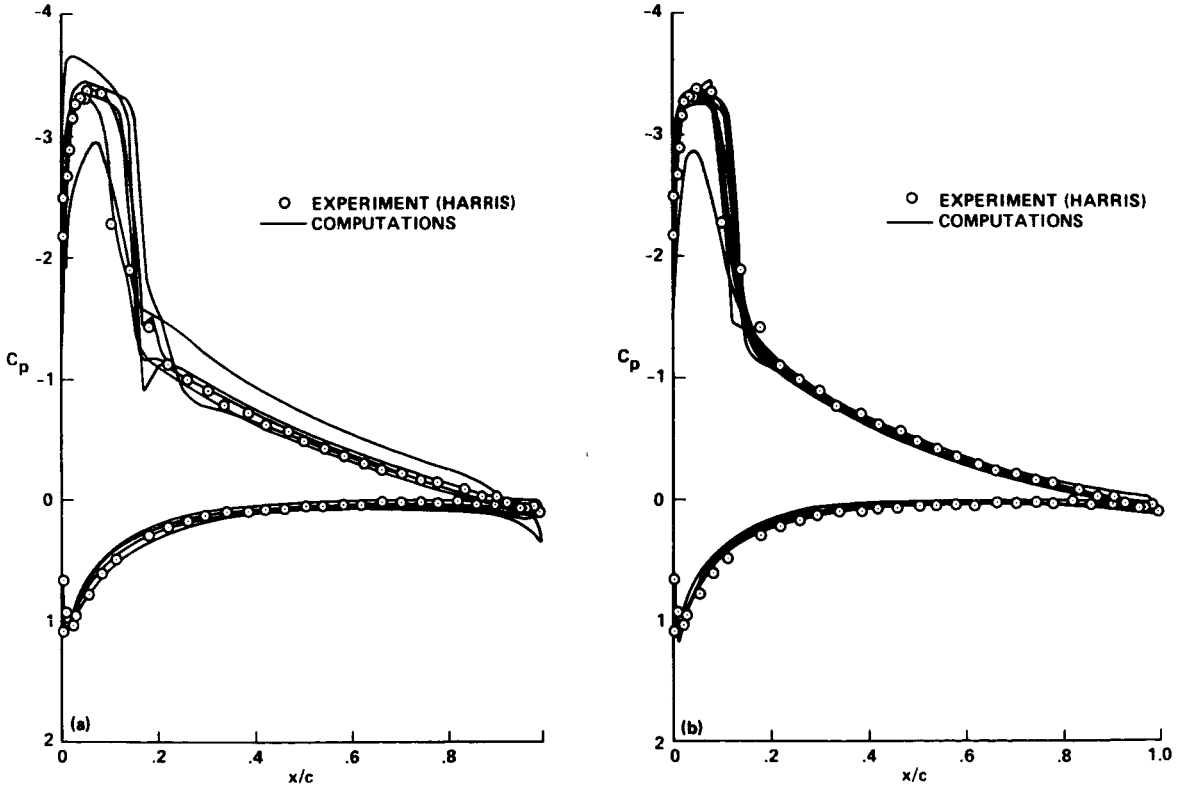

Fig. 2.- Comparison of pressure coefficient distributions for the NACA 0012 airfoil, $M_\infty = 0.55$, $\alpha = 8.34°$ (corrected), $Re_c = 9.0 \times 10^6$. a) Computations utilizing inviscid-plus-boundary-layer methods. b) Computations utilizing Navier-Stokes methods.

Comparisons of pressure coefficient distributions for the third NACA 0012 airfoil case are displayed in Fig. 3. The flow conditions for this case are $M_\infty = 0.799$, $\alpha = 2.26°$, and $Re_c = 9x10^6$. Again, the computational angle of attack (2.26°) is obtained from the measured angle of attack (2.86°) using a linear wind-tunnel-wall correction procedure. For this flow field a shock wave exists on the airfoil upper surface at about $x/c = 0.5$, which is strong enough to cause significant boundary layer separation. This case represents a severe test for all methods. The results are divided into five groups as follows: a) computations utilizing inviscid-plus-boundary-layer methods (6 curves), b) computations utilizing Navier-Stokes methods on coarse grids (4 curves), c) computations utilizing Navier-Stokes methods on fine grids (5 curves), d) Navier-Stokes computations with turbulence model variation due to King (Ref. 10; 3 curves), and e) Navier-Stokes computations with turbulence model variation due to Coakley (Ref. 7; 4 curves). The coarse-grid Navier-Stokes results were computed on grids ranging from 127 x 32 to 193 x 49, and the fine-grid results ranged from 257 x 57 to 265 x 101.

The inviscid-plus-boundary-layer results (Fig. 3a) show a significant amount of scatter especially at the shock wave and on the lower surface. Nevertheless, several of these methods do a good job in predicting both the position and strength of the shock wave. The

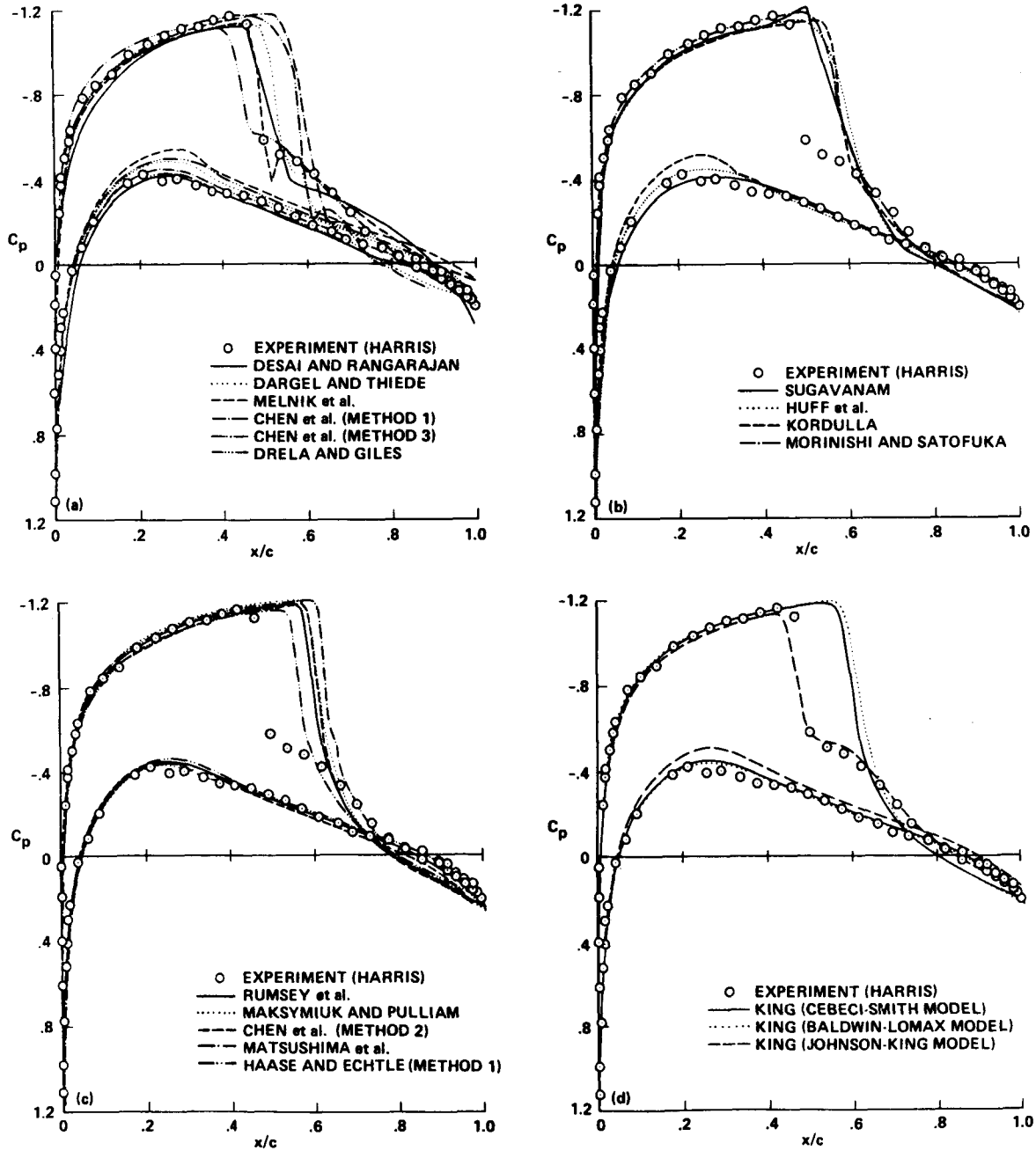

Fig. 3.- Comparison of pressure coefficient distributions for the NACA 0012 airfoil, $M_\infty = 0.799$, $\alpha = 2.26°$ (corrected), $Re_c = 9.0x10^6$. a) Computations utilizing inviscid-plus-boundary-layer methods. b) Computations utilizing Navier-Stokes methods on coarse grids. c) Computations utilizing Navier-Stokes methods on fine grids. d) Navier-Stokes computations with turbulence model variation due to King (Ref.10).

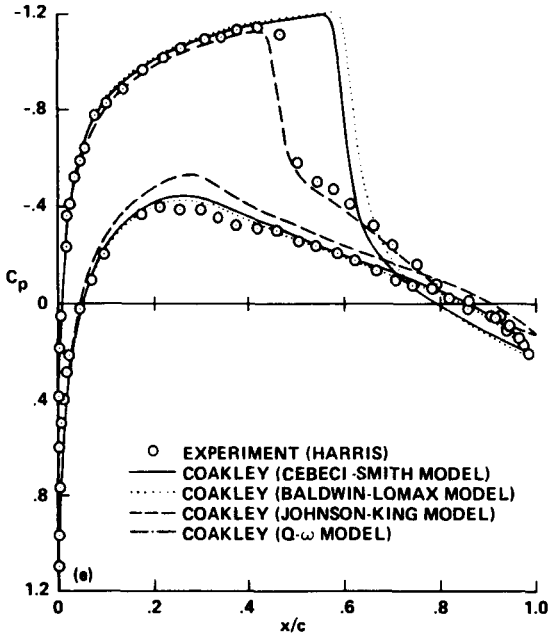

Fig. 3.- Concluded. e) Navier-Stokes computations with turbulence model variation due to Coakley (Ref.7).

coarse-grid Navier-Stokes results shown in Fig. 3b are generally in close agreement with each other but miss both the shock strength and position. The fine-grid Navier-Stokes results (Fig. 3c) are very similar to the coarse-grid results except the shock is slightly sharper. Thus, grid refinement is not the answer for obtaining good agreement for this case.

The turbulence model used in all but one of the nine.Navier-Stokes computations shown in Figs. 3b and 3c was the Baldwin-Lomax model (Ref. 20). In Fig. 3d King (Ref. 10) has computed results for three different turbulence models including Baldwin-Lomax, Cebeci-Smith (Ref. 21), and the newer Johnson-King model (Ref. 22). In Fig. 3e Coakley (Ref. 7) has computed results for four different turbulence models including Baldwin-Lomax, Cebeci-Smith, Johnson-King, and a two-equation model called Q-ω (Ref. 23). Note that the Q-ω and Cebeci-Smith results are identical and therefore are plotted as a single solid line. For the computations in Figs. 3d and 3e, only the turbulence model was allowed to vary, all other physical and numerical factors were held fixed. The Baldwin-Lomax, Cebeci-Smith, and Q-ω results from both codes produce results which are essentially identical to the other Navier-Stokes results (Figs. 3b and 3c). The shock is too strong and too far aft on the airfoil. However, the Johnson-King results are in excellent agreement at the shock, accurately predicting both shock position and strength. One drawback associated with the Johnson-King model computations is the under prediction of pressure on the airfoil lower surface. This, of course, will lead to a significant under prediction in lift relative to the experimental value. It is interesting to note that most of the inviscid-plus-boundary-layer results displayed in Fig. 3a, which agree well with the upper-surface shock strength and position, also under predict the lower-surface pressure distribution.

Figure 4 shows a comparison of 22 C_L vs α curves plotted without labels for the NACA 0012 airfoil at $M_\infty = 0.7$ and $Re_c = 9\text{x}10^6$. Experimental results from Harris with wind-tunnel-wall corrections included are also displayed. Most of the computed curves show good agreement with each other and with experiment at lower angles of attack. However, the overall comparison is disappointing at higher angles of attack. The scatter in the maximum lift value is particularly large. The $\alpha = 1.49°$ experimental point corresponds to the slightly-transonic solution shown in Fig. 1 where agreement is generally good. For angles of attack above this point the flow is more strongly transonic and eventually separates. In addition, several authors reported convergence difficulties or solution unsteadiness at these higher angles of attack. This may be a contributing factor to the large amount of scatter in the maximum C_L.

Drag polar comparisons are displayed in Fig. 5 for the NACA 0012 airfoil at $M_\infty = 0.7$ and $Re_c = 9\text{x}10^6$. As before, this set of comparisons is broken into several parts with experimental results of Harris included in each part for comparison. For $C_L \sim 0.2$ and lower, the flow field is subsonic. Drag values below this point correspond to pressure-plus-skin-friction drag and values above have, in addition, a wave-drag component. Since the pressure comparisons shown in Fig. 1 are all in good agreement, any disagreement in subcritical drag shown in Fig. 5 is probably due to disagreements in the skin-friction-drag component. However, since the pressure integration for drag can be quite sensitive, this ascertion should be studied in more detail by examining computed drag-component results.

Turbulence model variation has an effect on the drag polar as shown in Figs. 5e and 5f. For both figures, the newer Johnson-King turbulence model results overpredict the drag in comparison with experiment for the higher lift values, while the older models yield reasonable agreement. This trend is rather puzzling since the Johnson-King model yielded the best pressure distribution through the shock wave for the strongly separated case presented in Fig. 3. Perhaps the reason for poor drag polar agreement is associated with the under prediction of lower-surface pressure as predicted by the Johnson-King model in Figs. 3d and 3e. This would lower the lift, and if the drag is unaffected, produce the situation observed in Figs. 5e and 5f. However, several of the inviscid-plus-boundary-layer results

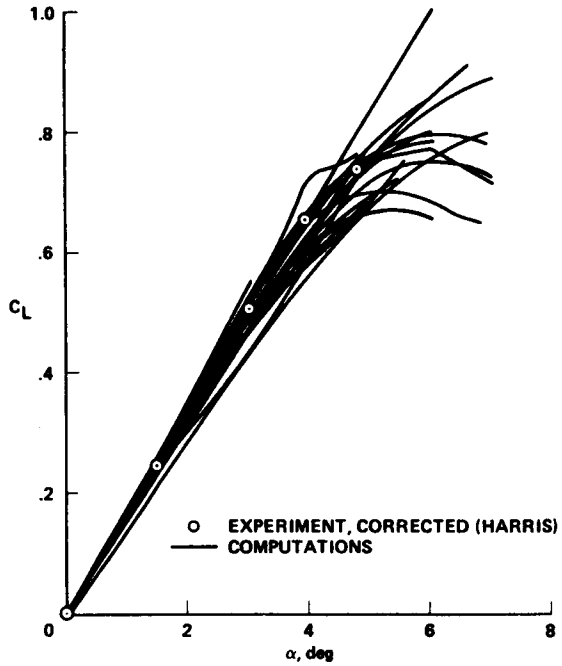

Fig. 4.- Comparison of lift coefficient versus angle of attack for the NACA 0012 airfoil, $M_\infty = 0.7$, $Re_c = 9.0 \times 10^6$.

presented in Figs. 5a and 5b also exhibit the same under prediction of pressure, but produce good drag polar results. This general area of drag prediction should be the subject of additional study.

Transonic drag-rise characteristics for the NACA 0012 airfoil at zero-lift conditions are displayed in Fig. 6. This set of comparisons is also broken into several parts and compared with a range of experimental data compiled by McCroskey (Ref. 24). All computations were performed at a Reynolds number based on airfoil chord of 9 million. The turbulent boundary layer was numerically "tripped" at $x/c = 0.05$ for those methods with trip or transition modeling and at the airfoil leading edge for those methods without. Each numerical curve shown in Fig. 6 is displayed with the computational points used to establish that curve (shown as solid circular symbols) when those points were available and when a small number of points (3 or 4) were used to establish the entire curve.

The range of experimental data displayed in Fig. 6 was established by looking at a large number of experiments (approximately 50). The six "best" sets of data, including Harris (Ref. 19), were selected, adjusted for Reynolds number effects, and plotted in Fig. 6 as a cross-hatched region. The different sets of experimental data, the selection process, and the Reynolds number adjustment procedure are

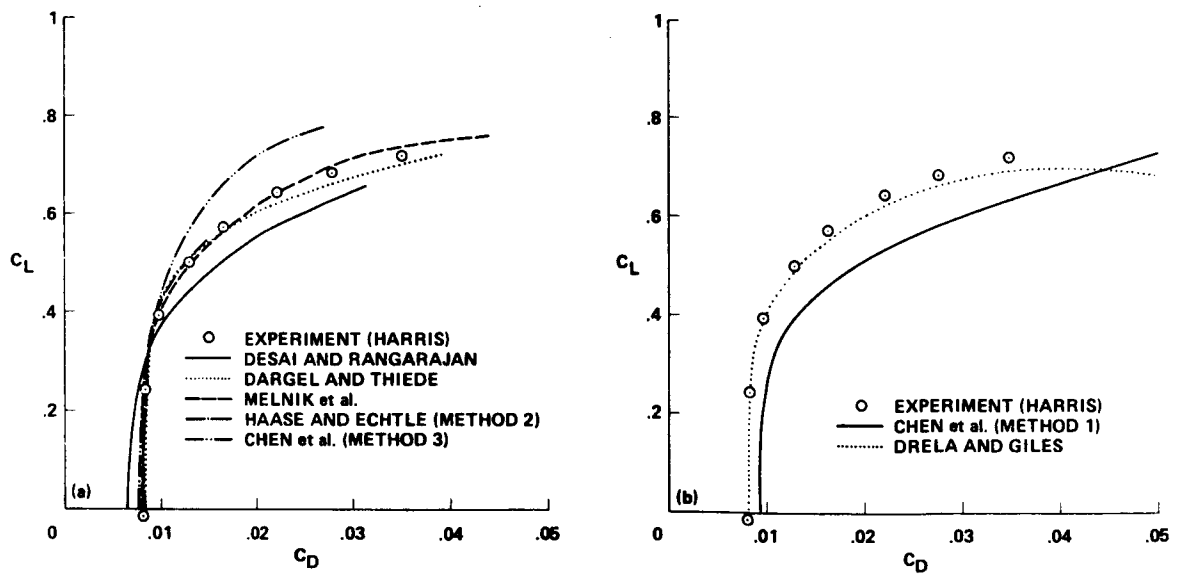

Fig. 5.- Comparison of lift versus drag polars for the NACA 0012 airfoil, $M_\infty = 0.7$, $Re_c = 9.0 \times 10^6$. a) Computations utilizing potential-plus-boundary-layer methods. b) Computations utilizing Euler-plus-boundary-layer methods.

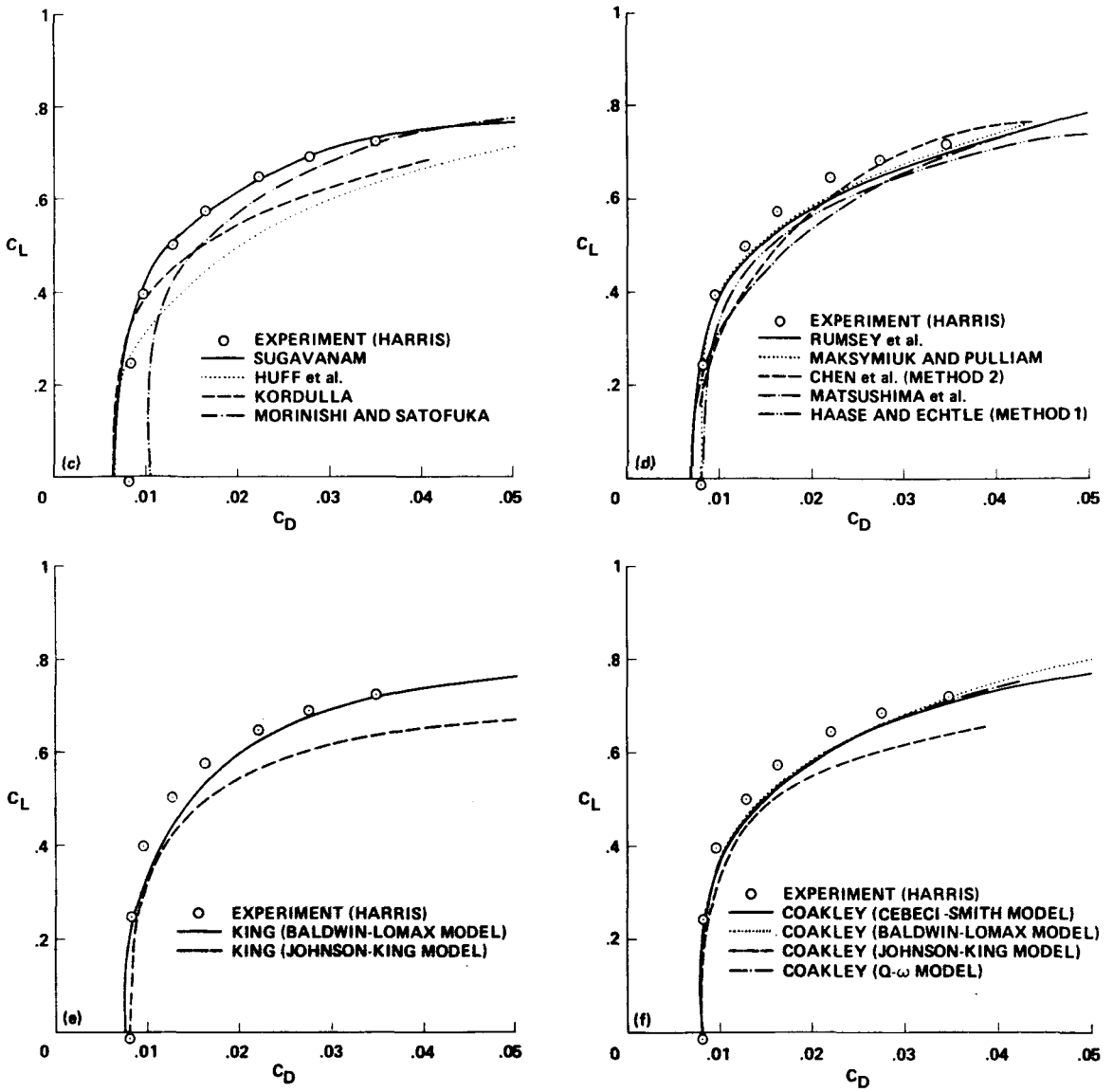

Fig. 5.- Concluded. c) Computations utilizing Navier-Stokes methods on coarse grids. d) Computations utilizing Navier-Stokes methods on fine grids. e) Navier-Stokes computations with turbulence model variation due to King (Ref. 10). f) Navier-Stokes computations with turbulence model variation due to Coakley (Ref.7).

described in McCroskey (Ref. 25). For this adjusted set of data, at a freestream Mach number of 0.7 the experimental drag value ranges from about 73 to 83 counts. For reference, Harris' highest Reynolds number tripped data produced a drag of about 75 counts.

The inviscid-plus-boundary-layer computations shown in Figs. 6a and 6b generally agree well with each other and with the experimental range of results. The drag-divergence Mach number is difficult to ascertain for some methods, especially the two Euler-plus-boundary-layer results shown in Fig. 6b. The scatter associated with the coarse-grid Navier-Stokes results (Fig. 6c) is quite large relative to the other computational and experimental results, especially at the subsonic Mach numbers, and suggests that the boundary layer grid refinement, or perhaps grid clustering, is a key parameter for drag calculations. The last two parts of Fig. 6 (Figs. 6e and 6f) show the effect of turbulence model variation on the drag-rise characteristics of the NACA 0012 airfoil. Except for relatively small variations in subsonic drag levels, there is virtually no variation in drag rise because of the turbulence models tested for this case.

Figure 7 shows computations (3 curves) compared with a range of experimental data, again compiled by McCroskey (Ref. 24), for the lift-curve slope ($dC_L/d\alpha$) plotted versus freestream Mach number. Values for $dC_L/d\alpha$ were obtained by computing the lift at $\alpha = 1.0°$. The units on $dC_L/d\alpha$ are therefore $(°)^{-1}$. This particular curve is significant because of its sensitivity to shock wave position and shock/boundary-layer interaction. The three computed results are in good agreement with the experimental range at lower free-stream Mach numbers, but deviate quickly. The single inviscid-plus-boundary-layer result starts deviation at about the drag-divergence Mach number. The two Navier-Stokes results qualitatively follow most of the experimental trends, including the severe shock-induced lift loss in the range $0.85 \leq M_\infty \leq 0.90$, but miss the appropriate levels, especially the minimum value of $dC_L/d\alpha$ at $M_\infty = 0.88$.

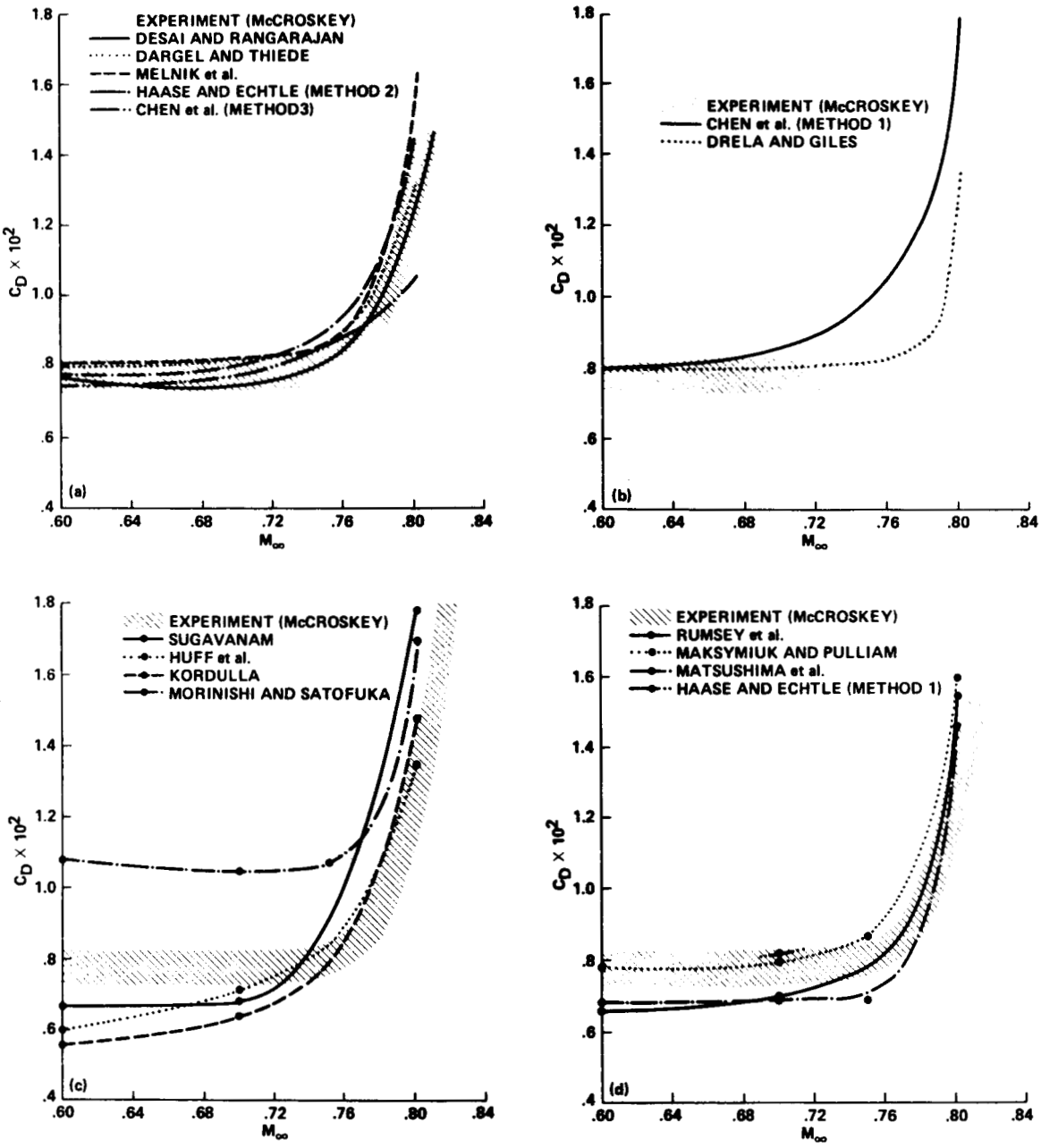

Fig. 6.- Comparison of computed and measured transonic drag-rise characteristics for the NACA 0012 airfoil, $\alpha = 0°$, $Re_c = 9.0 \times 10^6$. a) Computations utilizing potential-plus-boundary-layer methods. b) Computations utilizing Euler-plus-boundary-layer methods. c) Computations utilizing Navier-Stokes methods on coarse grids. d) Computations utilizing Navier-Stokes methods on fine grids.

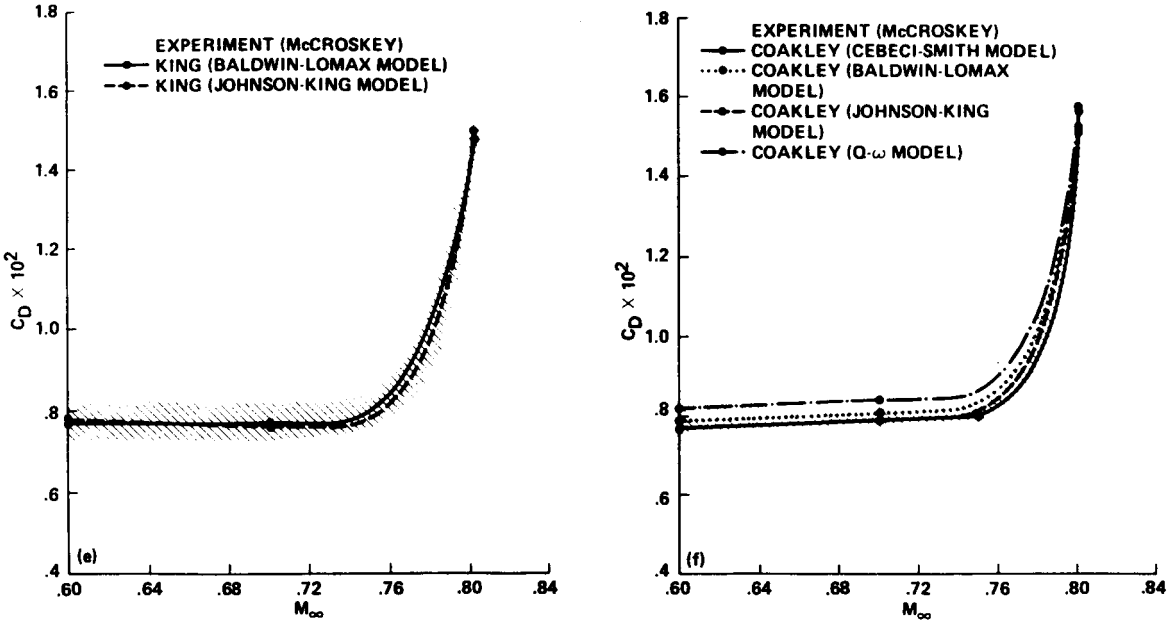

Fig. 6.- Concluded. e) Navier-Stokes computations with turbulence model variation due to King (Ref. 10). f) Navier-Stokes computations with turbulence model variation due to Coakley (Ref. 7).

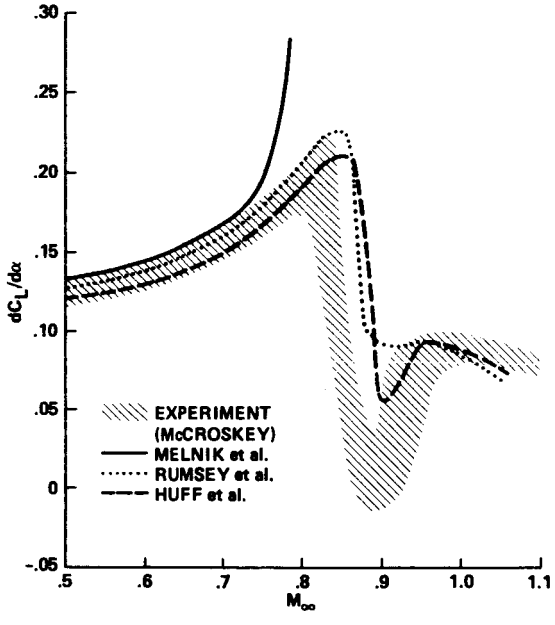

Fig. 7.- Comparison of computed and measured results for the lift-curve slope as a function of the freestream Mach number, NACA 0012 airfoil.

GRID REFINEMENT STUDY

As a part of the VTA Workshop, a grid refinement study was requested for the NACA 0012 airfoil solution presented in Fig. 1. The conditions for this solution are as follows: $M_\infty = 0.7$, $\alpha = 1.49°$, and $Re_c = 9\text{x}10^6$. This is a relatively easy solution with all CFD methods producing excellent agreement with each other and with experiment in terms of surface pressure (Fig. 1). Results of the grid refinement study are shown in Fig. 8 where the drag coefficient is plotted versus the inverse of the number of grid points on the airfoil chord (Δ). There are a total of six curves displayed in this figure, all without labels. The computational points defining each curve are displayed as solid circular symbols. The experimental drag level from Harris and a drag band representing the computational methods that reported drag levels for this case are also displayed. As desired, most of the curves approach a drag asymptote which falls in the lower end of the computational band near the experimental value ($C_D = 0.0079$). Of the curves presented, three have large slopes

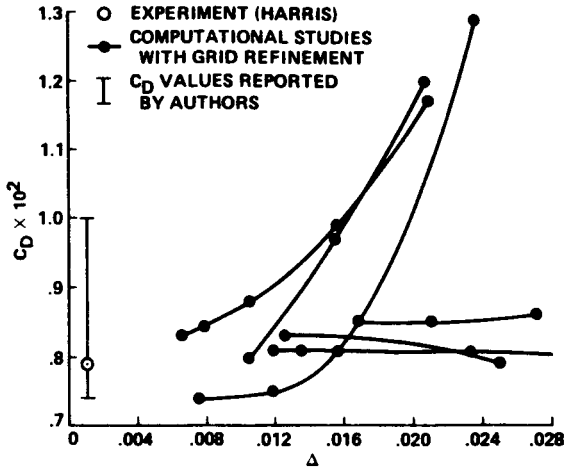

Fig. 8.- Computed drag coefficient versus average grid spacing on the airfoil upper surface (Δ) for the NACA 0012 airfoil (grid refinement study), $M_\infty = 0.7$, $\alpha = 1.49°$, $Re_c = 9.0 \times 10^6$.

and three have small slopes. The methods that produce small-slope results have reasonable drag levels even on coarse grids, which is a desirable characteristic. The methods that produce large-slope results have large drag errors when coarse grids are used. This is an alarming situation. Grid refinement checks such as the one in Fig. 8 are extremely important and can help calibrate the level of grid refinement required for applications and even uncover errors when the proper asymptotic behavior is not achieved.

COMPUTATIONAL STATISTICS

A relatively complete set of computational statistics for several of the cases just presented is given in Ref. 17. Of particular interest are the floating-point operation counts required for a solution from each of the individual methods. These statistics were not directly available from each author but were estimated from the statistics generally supplied by each author. The variation in per-solution operation count was quite large ranging from 4×10^7 to 6×10^{11}. The inviscid-plus-boundary-layer methods (Nos. 2, 3, 5, 11, 13, 20, and 22 from Table 1) have operation counts that range from about 4×10^7 to 2×10^{10}. This range is very large by itself and is primarily due to the wide diversity of methods within this category. The operation counts for the Navier-Stokes methods vary from about 2×10^{10} to 6×10^{11} and are due to variations in grid size and rates of convergence. From these statistics the inviscid-plus-boundary-layer methods appear to be about 30 to 500 times faster than the Navier-Stokes methods. However, caution should be exercised with this comparison because the Navier-Stokes methods generally utilized finer grids and produced most of the solutions for the more difficult cases, for example, cases involving maximum lift or drag. In addition, several of the Navier-Stokes methods were used time-accurately for unsteady solutions which increased the operation counts for these runs by several times.

CONCLUDING REMARKS

The Viscous Transonic Airfoil (VTA) Workshop has been held for the purpose of validating viscous transonic airfoil computations over a range of flow conditions. A total of 15 author groups have submitted 23 different sets of computed results. These results are compared with each other and experiment, when appropriate, in a series of plots with a variety of different results. The primary objective of this presentation is to establish method capabilities for predicting trends and individual flow field details. An additional purpose is the establishment of a data base which can be used for future computer code validation.

To a large extent the results obtained from the VTA Workshp are presented herein without concluding remarks. Specific conclusions about which methods are superior or inferior are left to the reader. Nevertheless, several general conclusions are easily identified and are now presented.

1. CFD methods for transonic, attached airfoil calculations have reached a sophisticated level of development. Most methods are capable of producing valuable results in the design environment, including the prediction of lift to within ±3% and drag to within ±5%. Other computed flow field data, including velocity boundary layer profiles and skin friction distributions, are in good agreement with each other and with experiment. Computational and experimental scatter for zero-lift drag-rise characteristics are comparable providing proper levels of grid refinement are utilized in obtaining the computational results.

2. CFD methods for transonic, separated airfoil calculations are not as well developed as the methods for attached flow computations. This is largely due to the lack of accurate turbulence modeling in regions of separated flow. Turbulence model inadequacies are the most important physical model error associated with the results contained in this report. Despite this major problem, recent progress in this area suggests hope for the future.

3. Many errors associated with CFD computer programs are solely numerical in nature. This type of error can be identified by various types of solution-to-solution comparison. Inappropriate grid clustering and refinement are the most important numerical errors associated with the results contained in this report. Establishment of "standard" levels of grid refinement is difficult because different methods have different requirements. However, grid refinement studies can be used to help eliminate these errors. More emphasis should be placed on solution-to-solution comparisons to aid in the evaluation and elimination of numerical errors.

ACKNOWLEDGMENTS

The time and effort of all the authors who participated in this workshop is deeply appreciated. Without their efforts an undertaking of this sort would not have been possible. In addition, the efforts of all the committee members who participated in the selection of test cases used in this workshop is deeply appreciated. A list of these individuals is as follows: Drs. Richard Barnwell, Leland Carlson, Norman Malmuth, Frank Marconi, Jr., William McCroskey, and William Van Dalsem.

REFERENCES

1. Sugavanam, A., "Transonic Viscous Flow Predictions with the Lockheed Navier-Stokes Code," AIAA Paper No. 87-0410, Jan. 1987.

2. Desai, S. S. and Rangarajan, R., "Viscous Tansonic Flow over Aerofoils Using Transonic Full Potential Equation in a System of Cartesian Coordinates," AIAA Paper No. 87-0411, Jan. 1987.

3. Dargel, G. and Thiede, P., "Viscous Transonic Airfoil Flow Simulation by an Efficient Viscous-Inviscid Interaction Method," AIAA Paper No. 87-0412, Jan. 1987.

4. Rumsey, C. L., Taylor, S. L., Thomas, J. L., and Anderson, W. K., "Application of an Upwind Navier-Stokes Code to Two-Dimensional Transonic Airfoil Flow," AIAA Paper No. 87-0413, Jan. 1987.

5. Melnik, R., Brook, J., and Mead, H., "GRUMFOIL: A Computer Code for the Computation of Viscous Transonic Flow Over Airfoils," AIAA Paper No. 87-0414, Jan. 1987.

6. Maksymiuk, C. M. and Pulliam, T. H., "Viscous Transonic Airfoil Workshop Results Using ARC2D," AIAA Paper No. 87-0415, Jan. 1987.

7. Coakley, T. J., "Numerical Simulation of Viscous Transonic Airfoil Flows," AIAA Paper No. 87-0416, Jan. 1987.

8. Chen, L. T., Li, S., and Chen, H., "Calculation of Transonic Airfoil Flows by Interaction of Euler and Boundary-Layer Equations," AIAA Paper No. 87-0521, Jan. 1987.

9. Chang, K. C., Alemdaroglu, N., Mehta, U., and Cebeci, T., "Further Comparisons of Interactive Boundary-Layer and Thin-Layer Navier-Stokes Procedures," AIAA Paper No. 87-0430, Jan. 1987.

10. King, L. S., "A Comparison of Turbulence Closure Models for Transonic Flows About Airfoils," AIAA Paper No. 87-0418, Jan. 1987.

11. Huff, D. L., Wu, J-C., and Sankar, L. N., "Analysis of Viscous Transonic Flow Over Airfoil Sections," AIAA Paper No. 87-0420, Jan. 1987.

12. Matsushima, K., Obayashi, S., and Fujii, K., "Navier-Stokes Computations of Transonic Flow Using the LU-ADI Method," AIAA Paper No. 87-0421, Jan. 1987.

13. Haase, W., Stock, H-W., and Echtle, H., "Computational Results for Some Test Cases of Viscous Transonic Flow Around Airfoils," AIAA Paper No. 87-0422, Jan. 1987.

14. Kordulla, W., "Using an Unfactored Predictor-Corrector Method," AIAA Paper No. 87-0423, Jan. 1987.

15. Drela, M. and Giles, M., "Viscous-Inviscid Analysis of Transonic and Low Reynolds Number Airfoils," AIAA Paper No. 87-0424, Jan. 1987.

16. Morinishi, K. and Satofuka, N., "A Numerical Study of Viscous Transonic Flows Using RRK Scheme," AIAA Paper No. 87-0426, Jan. 1987.

17. Holst, T. L., "Viscous Transonic Airfoil Workshop Compendium of Results," AIAA Paper No. 87-1640, June 1987.

18. Kline, S. J., Cantwell, B. J., and Lilley, G. M., Complex Turbulent Flows, Vol. II, 1980-81 AFOSR-HTTM-Stanford Conference on Complex Turbulent Flows, Stanford University, 1982.

19. Harris, C. D., "Two-Dimensional Aerodynamic Characteristics of the NACA 0012 Airfoil in the Langley 8-Foot Transonic Pressure Tunnel," NASA TM 81927, 1981.

20. Baldwin, B. S. and Lomax, H., "Thin Layer Approximation and Algebraic Model for Separated Turbulent Flows," AIAA Paper No. 78-0257, Jan. 1978.

21. Cebeci, T. and Smith, A. M. O., Analysis of Turbulent Boundary Layers, Academic Press, 1974.

22. Johnson, D. A. and King, L. S., "A Mathematically Simple Turbulence Closure Model for Attached and Separated Turbulent Boundary Layers," AIAA J., Vol. 23, No. 11, Nov. 1985, pp. 1684-1692.

23. Coakley, T. J., "Turbulence Modeling Methods for the Compressible Navier-Stokes Equations," AIAA Paper No. 83-1693, July 1983.

24. McCroskey, W. J., Private communication, October 1987.

25. McCroskey, W. J., "A Critical Assessment of Wind Tunnel Results for the NACA 0012 Airfoil," Paper No. 1, AGARD Fluid Dynamics Panel Symposium on Aerodynamic Data Accuracy and Quality: Requirements and Capabilities in Wind Tunnel Testing, Naples, Italy, Sept. 28-Oct. 2, 1987.

NASA
National Aeronautics and Space Administration

Report Documentation Page

1. Report No.	2. Government Accession No.	3. Recipient's Catalog No.
NASA TM-100095		

4. Title and Subtitle

Computational Fluid Dynamics Drag Prediction—Results from the Viscous Transonic Airfoil Workshop

5. Report Date

April 1988

6. Performing Organization Code

7. Author(s)

Terry L. Holst

8. Performing Organization Report No.

A-88142

10. Work Unit No.

505-60

9. Performing Organization Name and Address

Ames Research Center
Moffett Field, CA 94035

11. Contract or Grant No.

13. Type of Report and Period Covered

Technical Memorandum

12. Sponsoring Agency Name and Address

National Aeronautics and Space Administration
Washington, DC 20546-0001

14. Sponsoring Agency Code

15. Supplementary Notes

Point of Contact: Terry L. Holst, Ames Research Center, MS 258-1, Moffett Field, CA 94035
(415) 694-6032 or FTS 464-6032

16. Abstract

Results from the Viscous Transonic Airfoil Workshop held in January 1987, are compared with each other and with experimental data. Test cases used include attached and separated transonic flows for the NACA 0012 airfoil. A total of 23 sets of numerical results from 15 different author groups are included. The numerical methods used vary widely and include: 16 Navier-Stokes methods, 2 Euler/boundary-layer methods, and 5 potential/boundary-layer methods. The results indicate a high degree of sophistication among the numerical methods with generally good agreement between the various computed and experimental results for attached or moderately separated cases. The agreement for cases with larger separation is only fair and suggests additional work is required in this area.

17. Key Words (Suggested by Author(s))	18. Distribution Statement
Numerical analysis Transonic flow Viscous effects	Unclassified-Unlimited Subject Category – 02

19. Security Classif. (of this report)	20. Security Classif. (of this page)	21. No. of pages	22. Price
Unclassified	Unclassified	13	A02

For sale by the National Technical Information Service, Springfield, Virginia 22161